ARPN Journal of Engineering and Applied Sciences

INFLUENCE OF HEAT TRANSFER ON PERISTALTIC FLOW OF JEFFREY FLUID THROUGH A POROUS MEDIUM IN AN INCLINED ASYMMETRIC CHANNEL

G. Ravindranath Reddy[1], S. Ravikumar[2] and G. S. S. Raju[3]
[1]Department of Mathematics, Tadipatri Engineering College, Veerapuram, Tadipatri, India
[2]Department of Mathematics, N. B. K. R. Institute of Technology, Nellore, (A.P.), India
[3]Department of Mathematics, JNTUA College of Engineering Pulivendula, Pulivendula, (A.P.), India
E-Mail: ravindranathreddy.1982@gmail.com

ABSTRACT

In this paper, we studied the peristaltic flow of a Jeffrey fluid through a porous medium in an inclined asymmetric channel under the assumptions of long wavelength. The expressions for the velocity and pressure gradient are obtained analytically. The effects of various pertinent parameters on the pumping characteristics and temperature field are studied in detail with the aid of graphs.

Keywords: asymmetric channel, darcy number, froude number, jeffrey fluid, prandtl number.

1. INTRODUCTION

A lot of researchers imagined the fluid to behave similar to a Newtonian fluid for physiological peristalsis including the flow of blood in arterioles. But such a model cannot be suitable for blood flow unless the non - Newtonian nature of the fluid is incorporated in it. Chyme is undoubtedly a non-Newtonian fluid. Provost and Schwarz (1994) have explained a theoretical study of viscous effects in peristaltic pumping and assumed that the flow is free of inertial effects and that non-Newtonian normal stresses are negligible. In addition, the Jeffrey model is quite simpler linear model using time derivatives instead of convected derivatives, for example the Oldroyd-B model does, it represents rheology different from the Newtonian. In spite of its relative simplicity, the Jeffery model is able to specify the changes of the rheology on the peristalsis even under the assumption of long wavelength, low Reynolds number and small or large amplitude ratio. Hayat *et al*. (2006) investigated the effect of endoscope on the peristaltic flow of a Jeffrey fluid in a tube. Nagendra *et al*. (2008) have studied the peristaltic flow of a Jeffrey fluid in a tube.

A large amount attention has been curbed to symmetric channels or tubes, but there exist also flows which could not be symmetric. An example for a peristaltic type motion is the intra-uterine fluid flow due to momentarily contraction, where the myometrial contractions may occur in both symmetric and asymmetric directions. An interesting study was made by Eytan and Elad (1999), whose results have been used to analyze the fluid flow pattern in a non-pregnant uterus. In another paper, Eytan *et al*. (2001) discussed the characterization of non-pregnant women uterine contractions as they are composed of variable amplitudes and a range of different wave lengths. Mishra and Ramachandra Rao (2003) have investigated the peristaltic flow of a Newtonian fluid in an asymmetric channel. Elshewey *et al.* (2006) have analyzed the peristaltic flow of a Newtonian fluid through a porous medium in an asymmetric channel. Peristaltic transport of a power law fluid in an asymmetric channel was investigated by Subba Reddy *et al*. (2007). Navaneeswara Reddy *et al.* (2012) have investigated the peristaltic flow of a Prandtl fluid through a porous medium in a channel. Subba Reddy and Nadhamuni Reddy (2014) have studied the peristaltic flow of a non-Newtonian fluid through a porous medium in a tube with variable viscosity using Adomian decomposition method.

The study of heat transfer analysis is another important area in connection with peristaltic motion, which has industrial applications like sanitary fluid transport, blood pumps in heart lungs machine and transport of corrosive fluids where the contact of fluid with the machinery parts are prohibited. There are only a limited number of research available in literature in which peristaltic phenomenon has discussed in the presence of heat transfer (Mekheimer, Elmaboud, 2007; Vajravelu *et al*., 2007; Radhakrishnamacharya and Srinivasulu, 2007; Srinivas, Kothandapani, 2008; vasudev *et al*., 2010).

However, the flow of a Jeffrey fluid through a porous medium in an inclined asymmetric channel with peristalsis has received diminutive attention. Hence, an attempt is made to study the peristaltic flow of a Jeffrey fluid through a porous medium in an inclined asymmetric channel under the assumptions of long wavelength. The expressions for the velocity and pressure gradient are obtained analytically. The effects of various pertinent parameters on the pumping characteristics and temperature field are studied in detail with the aid of graphs.

2. MATHEMATICAL FORMULATION

We consider the flow of an incompressible Jeffrey fluid through a porous medium in an inclined asymmetric channel induced by sinusoidal wave trains propagating with constant speed c along the channel walls. The channel walls are inclined at an angle α to the horizontal. The lower and upper walls of the channel are maintained at constant temperatures T_1 and T_0, respectively. Figure-1 shows the schematic diagram of the problem.

VOL. 12, NO. 9, MAY 2017 ISSN 1819-6608
ARPN Journal of Engineering and Applied Sciences

The channel walls are characterized by

$$Y = H_1(X,t) = d + b_1 \cos\frac{2\pi}{\lambda}(X - ct) \quad \text{(upper wall)} \qquad (1a)$$

$$Y = H_2(X,t) = -d - b_2 \cos\left(\frac{2\pi}{\lambda}(X - ct) + \theta\right) \quad \text{(lower wall)} \qquad (1b)$$

where b_1, b_2 are the amplitudes of the waves, λ is the wavelength, $2d$ is the width of the channel, q is the phase difference which varies in the range $0 £ q £ p$, $q = 0$ corresponds to a symmetric channel with waves out of phase and $q = p$ defines the waves with in phase.

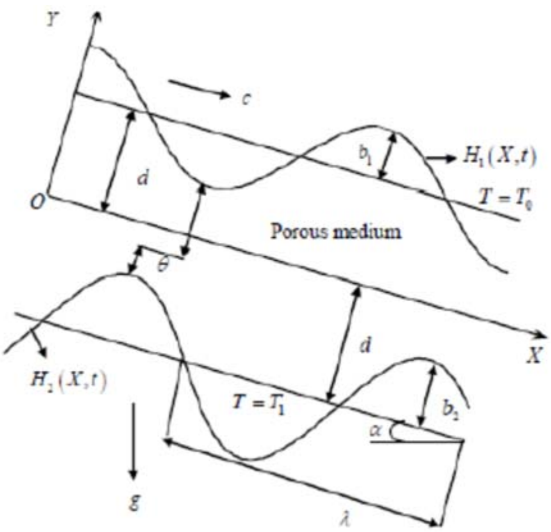

Figure-1. The physical model.

In fixed frame (X, Y), the flow is unsteady but if we choose moving frame (x, y), which travel in the X-direction with the same speed as the peristaltic wave, then the flow can be treated as steady.

The transformation between two frames are related by

$$x = X - ct, y = Y, u = U - c, v = V \text{ and } p(x) = P(X,t) \qquad (2)$$

where (u, v) and (U, V) are the velocity components, p and P are the pressures in wave and fixed frames of reference, respectively.

The pressure p remains a constant across any axial station of the channel, under the assumption that the wavelength is large and the curvature effects are negligible.

The constitutive equation for stress tensor t in Jeffrey fluid is

$$t = \frac{m}{1 + l_1}(g\&+ l\, g\&\&) \qquad (3)$$

where λ_1 is the ratio of relaxation time to retardation time, λ_2 is the retardation time, μ is the dynamic viscosity, $\dot{\gamma}$ is the shear rate and dots over the quantities indicate differentiation with respect to time t.

In the absence of an input electric field, the equations governing the flow field in a wave frame are

$$\frac{\partial u}{\partial x} + \frac{\partial v}{\partial y} = 0 \qquad (4)$$

$$\rho\left(u\frac{\partial u}{\partial x} + v\frac{\partial u}{\partial y}\right) = -\frac{\partial p}{\partial x} + \frac{\partial \tau_{xx}}{\partial x} + \frac{\partial \tau_{xy}}{\partial y} - \frac{\mu}{k_0}(u + c) + \rho g \sin\alpha \qquad (5)$$

$$\rho\left(u\frac{\partial v}{\partial x} + v\frac{\partial v}{\partial y}\right) = -\frac{\partial p}{\partial y} + \frac{\partial \tau_{yx}}{\partial x} + \frac{\partial \tau_{yy}}{\partial y} - \frac{\mu}{k}v - \rho g \cos\alpha \qquad (6)$$

$$\zeta\left[u\frac{\partial T}{\partial x} + v\frac{\partial T}{\partial y}\right] = \frac{k}{\rho}\nabla^2 T + v\left\{2\left[\left(\frac{\partial u}{\partial x}\right)^2 + \left(\frac{\partial v}{\partial y}\right)^2\right] + \left(\frac{\partial u}{\partial y} + \frac{\partial v}{\partial x}\right)^2\right\} \qquad (7)$$

where ρ is the density, k_0 is the permeability of the porous medium, ζ is the specific heat at constant volume, v is kinematic viscosity of the fluid, k is thermal conductivity of the fluid, g is the acceleration due to gravity, α is the inclination angle and T is temperature of the fluid.
The boundary conditions are

$$u = -c \text{ at } y = H_1, H_2 \qquad (8)$$

$$T = T_0 \text{ at } y = H_1 \qquad (9)$$

$$T = T_1 \text{ at } y = H_2 \qquad (10)$$

In order to write the governing equations and the boundary conditions in dimensionless form the following non - dimensional quantities are introduced.

$$\bar{x}=\frac{x}{\lambda};\bar{y}=\frac{y}{d};\bar{u}=\frac{u}{c},\bar{v}=\frac{v}{c\delta},\delta=\frac{d}{\lambda},\bar{p}=\frac{d^2p}{\mu c\lambda},\bar{t}=\frac{ct}{\lambda},h_1=\frac{H_1}{d},$$

$$h_2=\frac{H_2}{d},\phi_1=\frac{b_1}{d},\phi_2=\frac{b_2}{d},$$

$$\Theta=\frac{T-T_0}{T_1-T_0},\mathrm{Pr}=\frac{\rho\nu\zeta}{k},Ec=\frac{c^2}{\zeta(T_1-T_0)} \qquad (11)$$

where δ is the wave number and ϕ_1 and ϕ_2 are amplitude ratios.

In view of (11), the Equations (4) - (7), after dropping bars, reduce to

$$\frac{\partial u}{\partial x}+\frac{\partial v}{\partial y}=0 \qquad (12)$$

$$\mathrm{Re}\,\delta\left(u\frac{\partial u}{\partial x}+v\frac{\partial u}{\partial y}\right)=-\frac{\partial p}{\partial x}+\delta\frac{\partial\tau_{xx}}{\partial x}+\frac{\partial\tau_{xy}}{\partial y}-\frac{1}{Da}(u+1)+\frac{\mathrm{Re}}{Fr}\sin\alpha \qquad (13)$$

$$\mathrm{Re}\,\delta^3\left(u\frac{\partial v}{\partial x}+v\frac{\partial v}{\partial y}\right)=-\frac{\partial p}{\partial y}+\delta^2\frac{\partial\tau_{yx}}{\partial x}+\delta\frac{\partial\tau_{yy}}{\partial y}-\frac{\delta^2}{Da}v-\delta\frac{\mathrm{Re}}{Fr}\cos\alpha \qquad (14)$$

$$\mathrm{Re}\,\delta\left[u\frac{\partial\Theta}{\partial x}+v\frac{\partial\Theta}{\partial y}\right]=\frac{1}{\mathrm{Pr}}\left(\delta^2\frac{\partial^2\Theta}{\partial x^2}+\frac{\partial^2\Theta}{\partial y^2}\right)$$
$$+Ec\left\{4\delta^2\left(\frac{\partial u}{\partial x}\right)^2+\left(\frac{\partial u}{\partial y}\right)^2+\delta^4\left(\frac{\partial v}{\partial x}\right)^2+2\delta^2\frac{\partial u}{\partial y}\frac{\partial v}{\partial x}\right\} \qquad (15)$$

where $\mathrm{Re}=\frac{\rho dc}{\mu}$ is the Reynolds number, $Fr=\frac{c^2}{gd}$ is the Froude number, $Da=\frac{k_0}{d^2}$ is the Darcy number,

$$\tau_{xx}=\delta\frac{2}{(1+\lambda_1)}\left[1+\frac{\lambda_2 c\delta}{a_1}\left(u\frac{\partial}{\partial x}+v\frac{\partial}{\partial y}\right)\right]\frac{\partial u}{\partial x},$$

$$\tau_{xy}=\frac{1}{(1+\lambda_1)}\left[1+\frac{\lambda_2 c\delta}{a_1}\left(u\frac{\partial}{\partial x}+v\frac{\partial}{\partial y}\right)\right]\left(\frac{\partial u}{\partial y}+\delta^2\frac{\partial v}{\partial x}\right),$$

and $\tau_{yy}=\frac{2\delta}{(1+\lambda_1)}\left[1+\frac{\lambda_2 c\delta}{a_1}\left(u\frac{\partial}{\partial x}+v\frac{\partial}{\partial y}\right)\right]\frac{\partial v}{\partial y}$.

Under the assumptions of long wave length $(\delta<<1)$, the Equations (13) - (15) become

$$\frac{\partial p}{\partial x}=\frac{1}{1+\lambda_1}\frac{\partial^2 u}{\partial y^2}-\frac{1}{Da}(u+1)+\frac{\mathrm{Re}}{Fr}\sin\alpha \qquad (16)$$

$$\frac{\partial p}{\partial y}=0 \qquad (17)$$

$$\frac{1}{Pr}\left[\frac{\partial^2\Theta}{\partial y^2}\right]+Ec\left[\frac{\partial u}{\partial y}\right]^2=0 \qquad (18)$$

The non-dimensional boundary conditions are

$$u=-1 \text{ at } y=h_1,h_2 \qquad (19)$$

$$\Theta=0 \text{ at } y=h_1(x) \qquad (20)$$

$$\Theta=1 \text{ at } y=h_2(x) \qquad (21)$$

Equation (17) implies that $p\neq p(y)$, hence p is only function of x. Therefore, the Equation (16) can be rewritten as

$$\frac{dp}{dx}=\frac{1}{1+\lambda_1}\frac{\partial^2 u}{\partial y^2}-\frac{1}{Da}(u+1)+\frac{\mathrm{Re}}{Fr}\sin\alpha \qquad (22)$$

The rate of volume flow rate through each section in a wave frame, is calculated as

$$q=\int_{h_2}^{h_1}u\,dy \qquad (23)$$

The flux at any axial station in the laboratory frame is

$$Q(x,t)=\int_{h_2}^{h_1}(u+1)dy=q+h_1-h_2 \qquad (24)$$

The average volume flow rate over one period (T= λ/c) of the peristaltic wave is defined as

$$\bar{Q}=\frac{1}{T}\int_0^T Q\,dt=q+2 \qquad (25)$$

The dimensionless pressure rise per one wavelength in the wave frame is defined as

$$\Delta p = \int_0^1 \frac{dp}{dx} dx \tag{26}$$

3. SOLUTION

Solving Equation (22) using boundary conditions (19), we get

$$u = \left(\frac{1+\lambda_1}{\beta^2}\right)\left(\frac{dp}{dx} - \frac{\mathrm{Re}}{Fr}\sin\alpha\right)\left[c_1\cosh\beta y + c_2\sinh\beta y - 1\right] - 1 \tag{27}$$

where

$\beta^2 = (1+\lambda_1)\dfrac{1}{Da}$, $c_1 = \dfrac{\sinh\beta h_2 - \sinh\beta h_1}{\sinh\beta(h_2 - h_1)}$ and $c_2 = \dfrac{\cosh\beta h_1 - \cosh\beta h_2}{\sinh\beta(h_2 - h_1)}$.

Substituting Equation (27) in the Equation (18) and Solving Equation (18) using the boundary conditions (20) and (21), we obtain

$$\Theta = c_3 + c_4 y - E\,\mathrm{Pr}\frac{(1+\lambda_1)^2}{(8\beta^4)}\left(\frac{dp}{dx} - \frac{\mathrm{Re}}{Fr}\sin\alpha\right)^2 \begin{bmatrix} (c_1^2 + c_2^2)\cosh 2\beta y \\ +2c_1c_2\sinh 2\beta y \\ +2(c_2^2 - c_1^2)y^2 \end{bmatrix} \tag{28}$$

where

$c_3 = -c_4 h_1 + \dfrac{E\,\mathrm{Pr}\,c_5}{8N^4}(1+\lambda_1)^2\left(\dfrac{dp}{dx} - \dfrac{\mathrm{Re}}{Fr}\sin\alpha\right)^2$,

$c_4 = \dfrac{1}{h_2 - h_1} + \dfrac{E\,\mathrm{Pr}(c_6 - c_5)(1+\lambda_1)^2}{8(h_2 - h_1)N^4}\left(\dfrac{dp}{dx} - \dfrac{\mathrm{Re}}{Fr}\sin\alpha\right)^2$,

$c_5 = (c_1^2 + c_2^2)\cosh 2\beta h_1 + 2c_1c_2\sinh 2\beta h_1 + 2(c_2^2 - c_1^2)h_1^2$,

and $c_6 = (c_1^2 + c_2^2)\cosh 2\beta h_2 + 2c_1c_2\sinh 2\beta h_2 + 2(c_2^2 - c_1^2)h_2^2$.

The volume flow rate q in the wave frame of reference is given by

$$q = \left(\frac{1+\lambda_1}{\beta^3}\right)\left(\frac{dp}{dx} - \frac{\mathrm{Re}}{Fr}\sin\alpha\right)\frac{\begin{pmatrix} 2 - 2\cosh\beta(h_1 - h_2) \\ -\beta(h_1 - h_2)\sinh\beta(h_2 - h_1) \end{pmatrix}}{\sinh\beta(h_2 - h_1)} - (h_1 - h_2) \tag{29}$$

From (3.3), we have

$$\frac{dp}{dx} = \frac{\beta^3(q + h_1 - h_2)\sinh\beta(h_2 - h_1)}{(1+\lambda_1)\left(2 - 2\cosh\beta(h_1 - h_2) - \beta(h_1 - h_2)\sinh\beta(h_2 - h_1)\right)} + \frac{\mathrm{Re}}{Fr}\sin\alpha \tag{30}$$

The dimensionless pressure rise per one wavelength in the wave frame are defined as

$$\Delta p = \int_0^1 \frac{dp}{dx} dx \tag{31}$$

4. DISCUSSION OF THE RESULTS

In order to get the physical imminent of the problem, pumping characteristics and temperature field are computed numerically for different values of various emerging parameters are presented in Figures 2-15.

Figure-2 depicts the variation of pressure rise Δp with $\overline{Q}$ for different values of λ_1 with $\mathrm{Re} = 10, Fr = 2, \phi_1 = 0.5, \phi_2 = 0.7, Da = 0.1$, $\theta = \dfrac{\pi}{4}$, and $\alpha = \dfrac{\pi}{4}$. It is observed that, the $\overline{Q}$ decreases with increases λ_1 in the pumping region, whereas the $\overline{Q}$ increases in both the free pumping and co-pumping regions with increasing λ_1.

The variation of pressure rise Δp with $\overline{Q}$ for different values of θ with $\mathrm{Re} = 10$, $Fr = 2$, $\phi_1 = 0.5, \phi_2 = 0.7$, $Da = 0.1$, $\lambda_1 = 0.3$, and $\alpha = \dfrac{\pi}{4}$ is depicted in Figure-3. It is found that, the $\overline{Q}$ decreases with increasing phase shift θ in all the three regions, vz., pumping region $(\Delta p > 0)$, free pumping region $(\Delta p = 0)$ and co-pumping region $(\Delta p < 0)$. Moreover, the $\overline{Q}$ increases with increasing θ for appropriately chosen $\Delta p(< -10)$.

Figure-4 shows the variation of pressure rise Δp with $\overline{Q}$ for different values of Da with

ARPN Journal of Engineering and Applied Sciences

$\mathrm{Re}=10, Fr=2, \phi_1=0.5, \phi_2=0.7$, $\theta=\frac{\pi}{4}$, $\lambda_1=0.3$, and $\alpha=\frac{\pi}{4}$. It is noted that, in the pumping region $(\Delta p>0)$, the $\overline{Q}$ decreases with increasing Da whereas it increases with Da in both free pumping $(\Delta p=0)$ and co-pumping $(\Delta p<0)$ regions.

The variation of pressure rise Δp with $\overline{Q}$ for different values of ϕ_1 with $\mathrm{Re}=10, Fr=2$, $Da=0.1, \phi_2=0.7$, $\theta=\frac{\pi}{4}$, $\lambda_1=0.3$, and $\alpha=\frac{\pi}{4}$ is shown in Figure-5. It is found that, the $\overline{Q}$ increases with an increase in ϕ_1 in both pumping and free pumping regions. But in the co-pumping region, the $\overline{Q}$ decreases with increasing ϕ_1, for an appropriately chosen $\Delta p(<0)$.

Figure-6 illustrates the variation of pressure rise Δp with $\overline{Q}$ for different values of ϕ_2 with $\mathrm{Re}=10, Fr=2, \phi_1=0.5, Da=0.1$, $\theta=\frac{\pi}{4}$, $\lambda_1=0.3$, and $\alpha=\frac{\pi}{4}$. It is noted that, as ϕ_2 increases, the $\overline{Q}$ increases in both pumping and free pumping regions, while in co-pumping region, the $\overline{Q}$ decreases as ϕ_2 increases, for an appropriately chosen $\Delta p(<0)$.

The variation of pressure rise Δp with $\overline{Q}$ for different values of α with $\mathrm{Re}=10, Fr=2$, $\phi_1=0.5, \phi_2=0.7, \theta=\frac{\pi}{4}$, $\lambda_1=0.3$, and $Da=0.1$ is shown in Figure-7. It is found that, the $\overline{Q}$ increases in all the pumping, free pumping and co-pumping regions with an increase in α. Further, it is found that the $\overline{Q}$ is more for vertical channel than that of Horizontal channel.

Figure-8 depicts the variation of pressure rise Δp with $\overline{Q}$ for different values of Re with $Da=0.1, Fr=2, \phi_1=0.5, \phi_2=0.7, \theta=\frac{\pi}{4}$, $\lambda_1=0.3$, and $\alpha=\frac{\pi}{4}$. It is observed that, the $\overline{Q}$ increases in all the pumping, free pumping and co-pumping regions with increasing Re.

The variation of pressure rise Δp with $\overline{Q}$ for different values of Fr with $Da=0.1, \mathrm{Re}=10$, $\phi_1=0.5, \phi_2=0.7$, $\theta=\frac{\pi}{4}$, $\lambda_1=0.3$, and $\alpha=\frac{\pi}{4}$ is shown in Figure-9. It is noted that, the $\overline{Q}$ decreases in all the pumping, free pumping and co-pumping regions with an increase in Fr.

Figure-10 shows the temperature profiles for different values of λ_1 with $Fr=2$, $\theta=\frac{\pi}{4}$, $\phi_1=0.5, \phi_2=0.7$, $\mathrm{Re}=10$, $Da=0.1$, $q=-1$, $x=0.2$, $\alpha=\frac{\pi}{4}$ and $\Pr E=1$. It is found that, the Θ increases with increasing λ_1.

Temperature profiles for different values of phase shift θ with $Da=0.1$, $Fr=2$, $\phi_1=0.5, \phi_2=0.7$, $\mathrm{Re}=10$, $\lambda_1=0.3$, $q=-1$, $x=0.2$, $\alpha=\frac{\pi}{4}$ and $\Pr E=1$ is shown in Figure-11. It is observed that, the Θ oscillates with increasing θ.

Figure-12 illustrates the temperature profiles for different values of Darcy number Da with $Fr=2$, $\theta=\frac{\pi}{4}$, $\phi_1=0.5, \phi_2=0.7$, $\mathrm{Re}=10$, $\lambda_1=0.3$, $q=-1$, $x=0.2$, $\alpha=\frac{\pi}{4}$ and $\Pr E=1$. It is observed that, the Θ decreases with increasing Da.

Temperature profiles for different values of ϕ_1 with $Fr=2$, $\theta=\frac{\pi}{4}$, $Da=0.1, \phi_2=0.7$, $\mathrm{Re}=10$, $\lambda_1=0.3$, $q=-1$, $x=0.2$, $\alpha=\frac{\pi}{4}$ and $\Pr E=1$ is shown in Figure-13. It is observed that, the Θ increases with increasing ϕ_1.

Figure-14 depicts the temperature profiles for different values of ϕ_2 with $Fr=2, \theta=\frac{\pi}{4}$, $\phi_1=0.5, Da=0.1, \mathrm{Re}=10$, $\lambda_1=0.3$, $q=-1$, $x=0.2$, $\alpha=\frac{\pi}{4}$ and $\Pr E=1$. It is observed that, the Θ increases with increasing ϕ_2.

ARPN Journal of Engineering and Applied Sciences

Temperature profiles for different values of $\Pr E$ with $Fr = 2$, $\theta = \frac{\pi}{4}$, $\phi_1 = 0.5, \phi_2 = 0.7$, $\text{Re} = 10$, $\lambda_1 = 0.3$, $q = -1$, $x = 0.2$, $Da = 0.1$ and $\alpha = \frac{\pi}{4}$ is depicted in Figure-15. It is observed that, the Θ increases with increasing $\Pr E$.

5. CONCLUSIONS

In this chapter, we investigated the effects of Heat transfer on the peristaltic flow of a Jeffrey fluid in inclined asymmetric channel under the assumptions of long wavelength. The expressions for the velocity filed and temperature field are obtained. It is found that, in the pumping region the time averaged flux $\overline{Q}$ increases with increasing $\phi_1, \alpha, \text{Re}$ and ϕ_2 while it decrease with increasing θ, λ_1, Fr and Da. It is observed that the temperature field Θ increases with increasing λ_1, ϕ_1, ϕ_2 and $\Pr E$, while it decreases with increasing Da. Whereas the temperature field Θ oscillates with increasing θ.

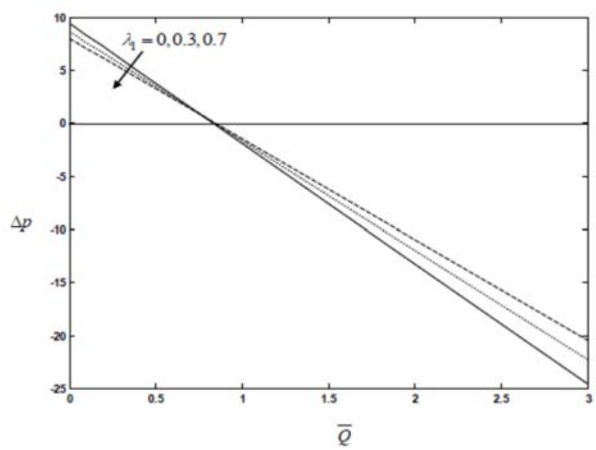

Figure-2. The variation of pressure rise Δp with $\overline{Q}$ for different values of λ_1 with $\text{Re} = 10, Fr = 2$, $\phi_1 = 0.5, \phi_2 = 0.7$, $Da = 0.1$, $\theta = \frac{\pi}{4}$, and $\alpha = \frac{\pi}{4}$.

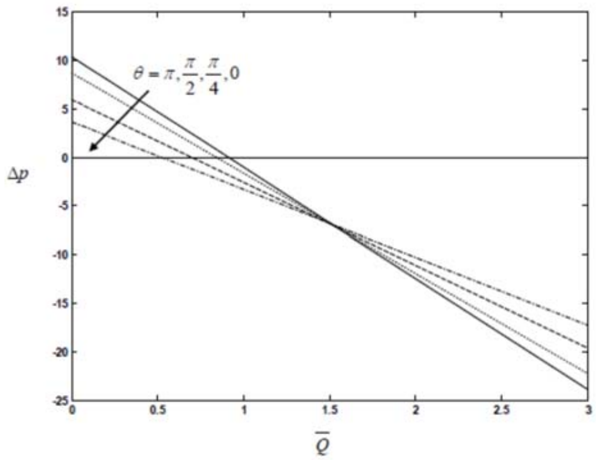

Figure-3. The variation of pressure rise Δp with $\overline{Q}$ for different values of θ with $\text{Re} = 10, Fr = 2$, $\phi_1 = 0.5, \phi_2 = 0.7$, $Da = 0.1$, $\lambda_1 = 0.3$, and $\alpha = \frac{\pi}{4}$.

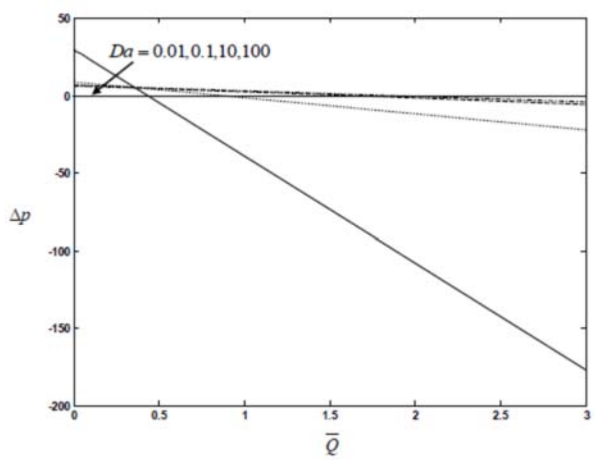

Figure-4. The variation of pressure rise Δp with $\overline{Q}$ for different values of Da with $\text{Re} = 10, Fr = 2$, $\phi_1 = 0.5, \phi_2 = 0.7$, $\theta = \frac{\pi}{4}$, $\lambda_1 = 0.3$, and $\alpha = \frac{\pi}{4}$.

ARPN Journal of Engineering and Applied Sciences

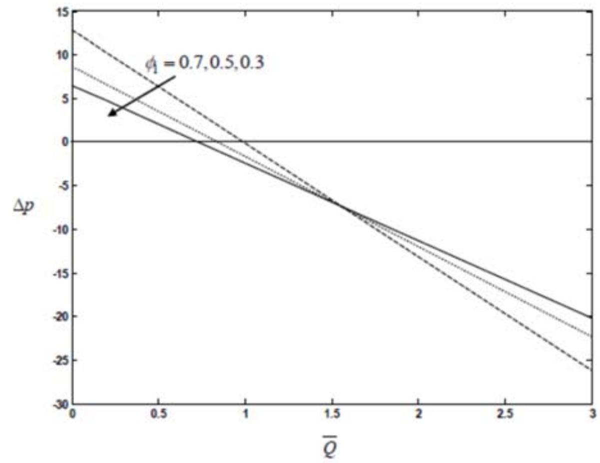

Figure-5. The variation of pressure rise Δp with $\overline{Q}$ for different values of ϕ_1 with $\mathrm{Re} = 10, Fr = 2$, $Da = 0.1, \phi_2 = 0.7$, $\theta = \dfrac{\pi}{4}$, $\lambda_1 = 0.3,$ and $\alpha = \dfrac{\pi}{4}$.

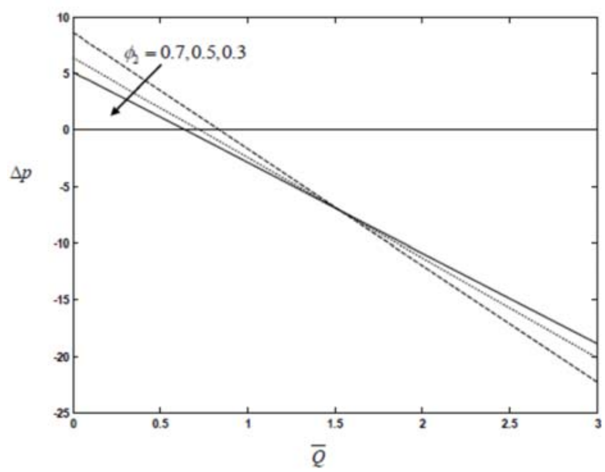

Figure-6. The variation of pressure rise Δp with $\overline{Q}$ for different values of ϕ_2 with $\mathrm{Re} = 10, Fr = 2$, $\phi_1 = 0.5, Da = 0.1$, $\theta = \dfrac{\pi}{4}$, $\lambda_1 = 0.3,$ and $\alpha = \dfrac{\pi}{4}$.

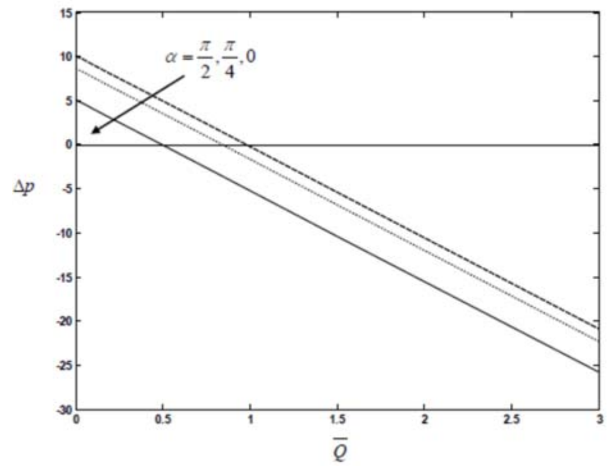

Figure-7. The variation of pressure rise Δp with $\overline{Q}$ for different values of α with $\mathrm{Re} = 10, Fr = 2$, $\phi_1 = 0.5, \phi_2 = 0.7$, $\theta = \dfrac{\pi}{4}$, $\lambda_1 = 0.3,$ and $Da = 0.1$.

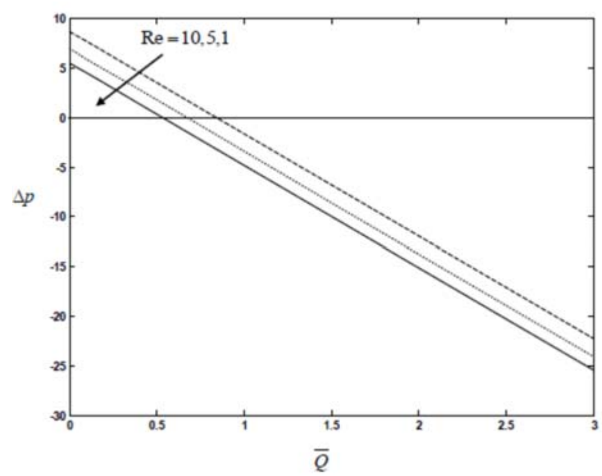

Figure-8. The variation of pressure rise Δp with $\overline{Q}$ for different values of Re with $Fr = 2$, $Da = 0.1$, $\phi_1 = 0.5, \phi_2 = 0.7$, $\theta = \dfrac{\pi}{4}$, $\lambda_1 = 0.3,$ and $\alpha = \dfrac{\pi}{4}$.

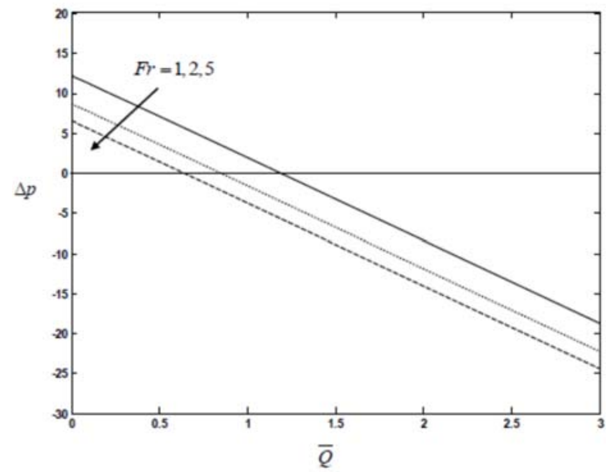

Figure-9. The variation of pressure rise Δp with $\overline{Q}$ for different values of Fr with $\mathrm{Re}=10$, $Da=0.1$, $\phi_1=0.5, \phi_2=0.7$, $\theta=\frac{\pi}{4}$, $\lambda_1=0.3$, and $\alpha=\frac{\pi}{4}$.

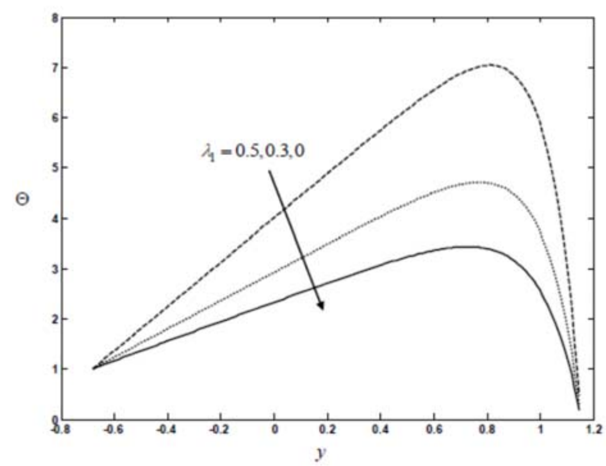

Figure-10. Temperature profiles for different values of λ_1 with $Fr=2$, $\theta=\frac{\pi}{4}$, $\mathrm{Re}=10$, $\phi_1=0.5, \phi_2=0.7$, $Da=0.1$, $q=-1$, $x=0.2$, $\alpha=\frac{\pi}{4}$ and $\Pr E=1$.

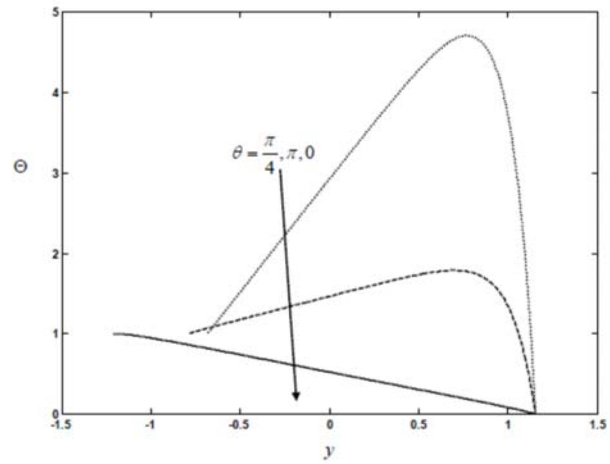

Figure-11. Temperature profiles for different values of phase shift θ with $Da=0.1$, $Fr=2$, $\phi_1=0.5, \phi_2=0.7$, $\mathrm{Re}=10$, $\lambda_1=0.3$, $q=-1$, $x=0.2$, $\alpha=\frac{\pi}{4}$ and $\Pr E=1$.

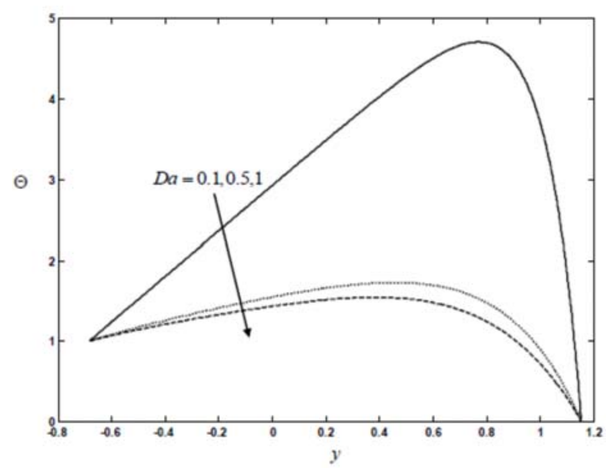

Figure-12. Temperature profiles for different values of Darcy number Da with $Fr=2$, $\theta=\frac{\pi}{4}$, $\phi_1=0.5, \phi_2=0.7$, $\mathrm{Re}=10$, $\lambda_1=0.3$, $q=-1$, $x=0.2$, $\alpha=\frac{\pi}{4}$ and $\Pr E=1$.

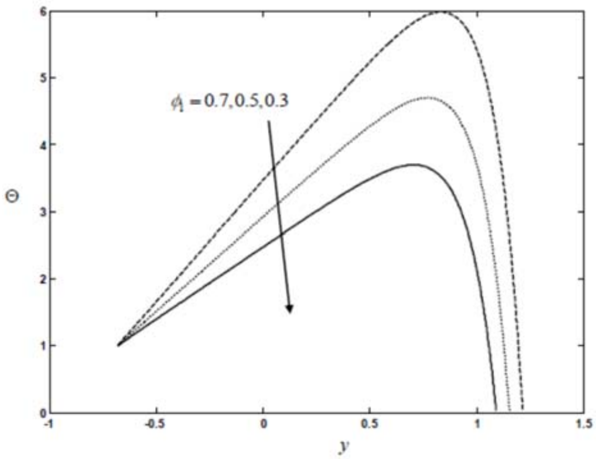

Figure-13. Temperature profiles for different values of ϕ_1 with $Fr = 2$, $\theta = \frac{\pi}{4}$, $\phi_2 = 0.7$, $Da = 0.1$, $\mathrm{Re} = 10$, $\lambda_1 = 0.3$, $q = -1$, $x = 0.2$, $\alpha = \frac{\pi}{4}$ and $\Pr E = 1$.

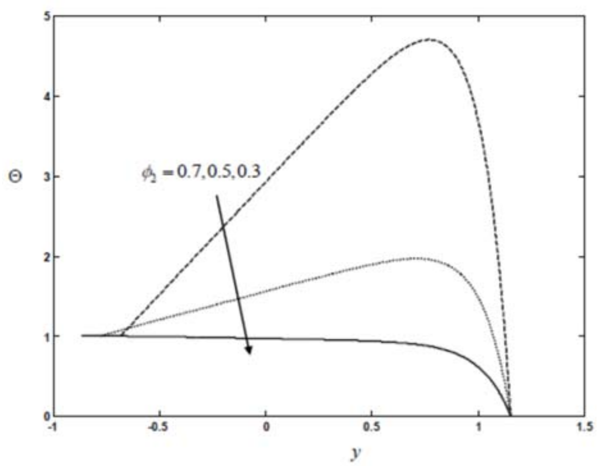

Figure-14. Temperature profiles for different values of ϕ_2 with $Fr = 2$, $\theta = \frac{\pi}{4}$, $\mathrm{Re} = 10$, $\phi_1 = 0.5, Da = 0.1$, $\lambda_1 = 0.3$, $q = -1$, $x = 0.2$, $\alpha = \frac{\pi}{4}$ and $\Pr E = 1$.

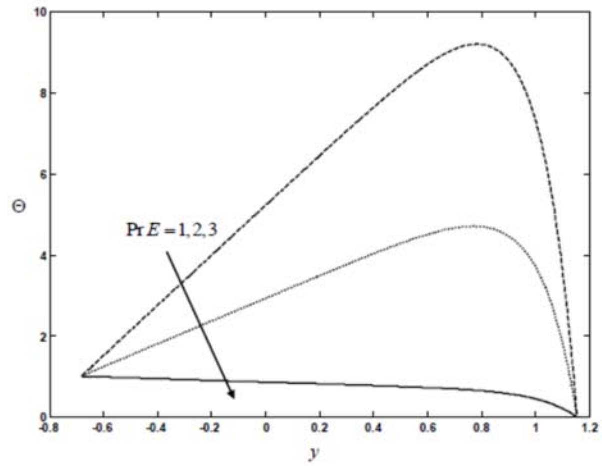

Figure-15. Temperature profiles for different values of $\Pr E$ with $Fr = 2$, $\theta = \frac{\pi}{4}$, $\mathrm{Re} = 10$, $\phi_1 = 0.5, \phi_2 = 0.7$, $\lambda_1 = 0.3$, $q = -1$, $x = 0.2$, $Da = 0.1$ and $\alpha = \frac{\pi}{4}$.

REFERENCES

EL Shehawey, E.F., Eldabe, N.T., Elghazy E.M. and Ebaid A. 2006. Peristaltic transport in an asymmetric channel through a porous medium, Appl. Math. Comput. 182: 140-150.

Eytan O. and Elad D. 1999. Analysis of Intra - Uterine fluid motion induced by uterine contractions, Bull. Math. Bio. 61: 221-238.

Eytan O., Jaffa A.J. and Elad D. 2001. Peristaltic flow in a tapered channel: application to embryo transport within the uterine cavity, Med. Engng. Phys. 23: 473-482.

Hayat T., Ali N., Asghar S. and Siddiqui A. M. 2006. Exact peristaltic flow in tubes with an endoscope, Appl. Math. Comput. 182: 359-368.

Mekheimer KhS, Abd elmaboud Y. 2007. The influence of heat transfer and magnetic field on peristaltic transport of a Newtonian fluid in a vertical annulus: application of an endoscope. Physics A. 1-9.

Mishra M. and Ramachandra RAO A. 2003. Peristaltic transport of a Newtonian fluid in an asymmetric channel, Z. Angew. Math. Phys. (ZAMP). 54: 532-550.

Nagendra N., Madhava Reddy N and Subba Reddy M. V. and Jayaraj B. 2008. Peristaltic flow of a Jeffrey fluid in a tube, Journal of Pure and Applied Physics. 20: 189-201.

Navaneeswara Reddy S., Viswanatha Reddy G. and Subba Reddy M. V. 2012. Peristaltic flow of a Prandtl fluid through a porous medium in a channel, Int. J. Mathematical Archive. 3(11): 4072-4080.

Provost A.M. and Schwarz W.H. 1994. A theoretical study of viscous effects in 15.peristaltic pumping, J. Fluid Mech. 279: 177-195.

Radhakrishnamacharya G and Srinivasulu Ch. 2007. Influence of wall properties on peristaltic transport with heat transfer. C R Mecanique. 335: 369-73.

Srinivas S, Kothandapani M. 2008. Peristaltic transport in an asymmetric channel with heat transfer, A note, Int. Communications in Heat and Mass Transfer. 35: 514-522.

Subba Reddy, M.V., Ramachandra Rao, A. and Sreenadh S. 2007. Peristaltic motion of a power law fluid in an asymmetric channel, Int. J. Non-Linear Mech. 42: 1153-1161.

Subba Reddy, M. V. and Nadhamuni Reddy C. 2014. Peristaltic flow of a non-Newtonian fluid through a porous medium in a tube with variable viscosity using Adomian decomposition method, International Review of Applied Engineering Research. 4(1): 137-146.

Vajravelu K, Radhakrishnamacharya G, Radhakrishnamurty V. 2007. Peristaltic flow and heat transfer in a vertical porous annulus with long wave approximation. Int. J. Nonlinear Mech. 42: 754-759.

Vasudev C., Rajeswara Rao U., Subba Reddy M. V. and Prabhakara Rao G. 2010. Influence of magnetic field and heat transfer on peristaltic flow of Jeffrey fluid through a porous medium in an asymmetric channel. ARPN Journal of Engineering and Applied Sciences. 5(12): 87-103.